Biophysical Chemistry 165–166 (2012) 74–78

Contents lists available at SciVerse ScienceDirect

Biophysical Chemistry

journal homepage: http://www.elsevier.com/locate/biophyschem

Importance of local interactions for the stability of inhibitory helix 1 in apo Ets-1

Aleksandra Karolak, Arjan van der Vaart *

Department of Chemistry, University of South Florida, 4202 East Fowler Avenue CHE 205, Tampa, FL 33620, United States

HIGHLIGHTS

- Simulation of Ets-1 constructs identified how HI-1 is stabilized in the apo state.
- Contacts between HI-1 and HI-2/H4 are important for the stability of HI-1.
- Removal of a few local contacts may lead to the partial unfolding of Ets-1.

GRAPHICAL ABSTRACT

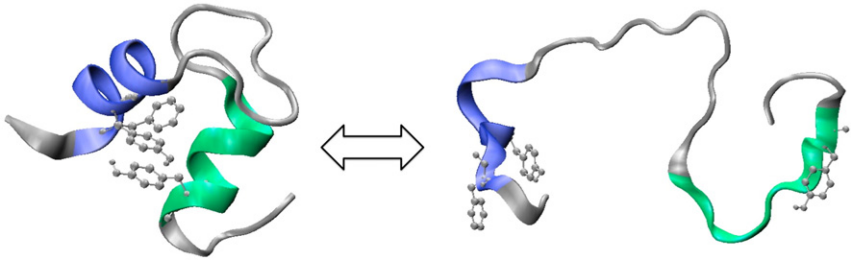

ARTICLE INFO

Article history:
Received 3 February 2012
Received in revised form 10 March 2012
Accepted 18 March 2012
Available online 23 March 2012

Keywords:
Ets-1
Transcription factor
Molecular dynamics simulation

ABSTRACT

Inhibitory helix 1 (HI-1) of the Ets-1 human transcription factor unfolds upon binding the target DNA sequence. To identify the interactions that stabilize HI-1 in the apo state, we performed replica exchange and molecular dynamics simulations of various apo Ets-1 constructs. The simulations indicate the importance of local interactions for the stability of HI-1. The HI-2 and H4 helices stabilize the helical state of HI-1 through specific residue–residue contacts and macrodipolar interactions. The amount of stabilization in small length HI-1 + H2 and HI-1 + H4 constructs was similar to that in the protein. The studies suggest that the partial unfolding of Ets-1 upon DNA binding can be achieved by the removal of just a few specific local contacts.

1. Introduction

The human Ets-1 transcription factor is important for embryonic development [1], apoptosis [2], and angiogenesis [3] in normal and pathological growth. Ets-1 is also involved in cancer metastasis and tumor progression. High expression levels in breast [4,5], ovary [6–8], and cervix [9] tumors correlate strongly with bad prognosis, while elevated expression is relevant for lung [10], colon [11], pancreatic [12,13], thyroid [13,14], and oral [15] cancers. In addition, Ets-1 plays a role in immunity and autoimmune diseases [16,17]. The protein consists of six domains [18]. The N-terminal domain contains a RAS-responsive phosphorylation site [19,20], which regulates the transcriptional activity of Ets-1. This domain is followed by the pointed domain, important for protein–protein interactions [21], the transactivation domain, important for transcription activation [22], and the D, ETS, and F domains which regulate DNA-binding [18,23].

DNA is bound by a winged helix-turn-helix motif in the ETS-domain (residues 331–415) [18]. This highly conserved domain binds the GGAA/T sequence in the major groove of purine-rich DNA by insertion of the recognition helix (H3). The minor groove is bound by a loop between β-sheets S3 and S4 and the turn between α-helices H2 and H3. The binding affinity for DNA is modulated by an auto-inhibitory module, which flanks the ETS domain and decreases the binding affinity of DNA 10 to 20 fold compared to the bare ETS domain [24]. The auto-inhibitory module consists of residues 301–330 of the D domain and residues 415–440 of the F domain [25–27]. These residues are folded into four α-helices: inhibitory helix 1 and 2 of the D domain (HI-1 and HI-2, respectively), and H4 and H5 of the F domain. The DNA-binding affinity is further regulated by calcium-dependent phosphorylation of an unstructured serine-rich region of the D domain (residues 243–300) [28], and by binding of protein partners like Runt-related transcription factor [23].

Abbreviations: MD, molecular dynamics; REX, replica exchange simulations.

* Corresponding author. Tel.: +1 813 974 8762; fax: +1 813 974 3203.
E-mail address: avandervaart@usf.edu (A. van der Vaart).

0301-4622/$ – see front matter © 2012 Elsevier B.V. All rights reserved.
doi:10.1016/j.bpc.2012.03.007

Autoinhibition is achieved by a highly unusual mechanism that involves the unfolding of HI-1 [18,23,27,29]. Previous studies in our laboratory have shown that the unfolding is due to a change in correlated motions between H4 and HI-1 [30]. In the apo protein, HI-1 and H4 move in a correlated fashion (in-phase; with positive covariances), and HI-1 is stabilized by hydrogen bonding and macrodipolar interactions with H4. In the DNA bound state, the motion between HI-1 and H4 is anti-correlated (out-of-phase; with negative covariances), which disrupts the macrodipolar and hydrogen bonding interactions. Computer simulations have shown that the change in correlated motions is due to hydrogen bonding between the amide backbone of Leu337 of H1 and the DNA [30]. This hydrogen bond was shown to act as a conformational switch in biochemical experiments as well [31,32]. Simulations showed that the conformational switch transfers the information that DNA is present to HI-1 by a network of correlated motions between H1, H4 and HI-1 [33].

Given the central role of HI-1 in the autoinhibition mechanism of Ets-1, we performed computer simulations to further investigate how HI-1 is stabilized in the apo state. Structural analyses show that HI-1 is loosely packed in the protein, making contacts with HI-2, H5 and H4 only. Moreover, experiments showed that HI-1 is marginally stable in the apo protein, may have unfavorable charge–charge interactions between Lys305 —Arg309 and Asp306-Asp310, and is conformationally dynamic on the milli to microsecond time scale [31]. Taken with our previous simulation data, these observations suggest that in the apo state, HI-1 is mostly stabilized by a few local contacts. The aim of our study was to establish the identity of these contacts, and to quantify which contribute most to the stabilization.

2. Materials and methods

Since no full-length structure of the Ets-1 protein exists, we used the NMR structure of the apo construct Δ301 (Ets-1 residues 301–440; Protein Data Bank entry 1R36 [31], Fig. 1) to generate all of our initial coordinates. This construct contains the ETS domain and the autoinhibitory module. Biochemical experiments have shown that the binding behavior of Δ301 is similar to the full-length protein, with unfolding of HI-1 upon specific DNA binding [27,31,34]. Several constructs were simulated: HI-1 (residues 301–314, Fig. 2A), HI-1 + HI-2 (residues 301–334, Fig. 2B), HI-1 + H4 (residues 304–310 and 418–422, Fig. 2C), and the Δ301 construct. HI-1 and H4 were fused in the HI-1 + H4 construct by a GT linker in order to mimic the nearly continuous HI-1-H4 helix that is observed in Δ301 [31]. The HI-1 + H4 construct was simulated in two ways: a simulation in which H4 was restrained to be α-helical, and a simulation in which no such restraints were used. These harmonic restraints were applied to the backbone of H4 with a force constant of 4.2 kJ/(mol Å^2). Several mutant constructs were simulated as well.

The simulations were performed using the CHARMM 19 [35] force field and FACTS implicit solvent model [36] as implemented in the CHARMM program [37]. FACTS was chosen because of its accuracy and performance; calculated solvation free energies on a set of 29 proteins closely matched those of Poisson-Boltzmann calculations at a fraction of the cost [36]. Langevin dynamics with a time step of 2 fs was used, and SHAKE [38] was applied to constrain bonds involving hydrogen atoms. To fully sample the conformational space, all constructs except Δ301 were simulated with temperature replica exchange (REX) [39]. In this method, identical copies of the system (replicas) are run at different temperatures. By frequently swapping the configurations based on a criterion that maintains detailed balance, much more configurational space can be sampled than in normal molecular dynamics (MD) simulations while maintaining thermodynamic equilibrium. Each REX simulation used 16 replicas at 200, 209, 219, 230, 241, 252, 264, 276, 289, 303, 317, 333, 348, 365, 382, 400 K. Selection of these temperatures was based on the calculated folding temperature (based on the calculated heat capacity of trial runs), and chosen to well cover the folded state and folding/unfolding transition and also to ensure good exchange between replicas. Since the simulations are performed in an implicit solvent model using a force field parameterized at room temperature, the folding temperature does not necessarily correspond to a physiological temperature. Coordinate swaps were attempted every 5 ps as a compromise between frequent exchange [40] and low parallel communication costs, and a total simulation time of 250 ns was used per replica to ensure convergence of all calculated properties. Since we were interested in the folding/unfolding of HI-1, and not in the folding/unfolding of the entire protein, REX could not be used for Δ301. Instead, we used four independent normal, unbiased MD runs for Δ301; each of 150 ns production length. All REX and MD systems were first heated for 500 ps with weak harmonic restraints on the backbone, followed by 500 ps of equilibration during which the harmonic restraints were gradually removed. For the fused HI-1 + H4 system in which H4 was restrained to be helical, only the restraints on HI-1 were gradually removed.

The secondary structure assignment was determined using the program STRIDE [41], and the output was used for the helical fraction (HF) calculations. HI-1 was considered folded when HF > 0.5. Free energy surfaces at 300 K were calculated using the weighted histogram analysis method (WHAM) using the data from all replicas [42,43]. These surfaces were based on the HF; surfaces for root mean square deviation, number of native contacts and radius of gyration gave similar results. WORDOM [44] was used for contact analysis. Dipoles were constructed using the N, H, CA, HA, C and O backbone atoms, and dipole–dipole interactions were calculated using standard methods [30]. All figures were generated using VMD [45] and povray (http://www.povray.org).

3. Results

Replica exchange simulations of the HI-1 construct showed a significant preference for the unfolded state, with the free energy of the unfolded state 3.2 kJ/mol lower than that of the folded state (Table 1). The higher stability of the unfolded state was not surprising, since the construct is short (14 residues) and helix formation generally takes more residues [46]. In addition to α-helical structures, the folded state structural ensemble also showed π-helical structures. Prevalent hydrophobic contacts were made between F304 and V308, and R309 with K305 (Fig. 3A and B). These contacts are also prevalent in Δ301, and help to stabilize the helix.

The HI-1 unfolded state consisted of a large ensemble of partially structured loops. Many of these structures had one helical turn or incomplete helical turns, while partial sheet structures were also observed. Structural analyses of the unfolded state showed the prevalence of a hydrophobic contact between F304 and R309 that did not occur in the folded state (Fig. 3C). In the unfolded state this contact

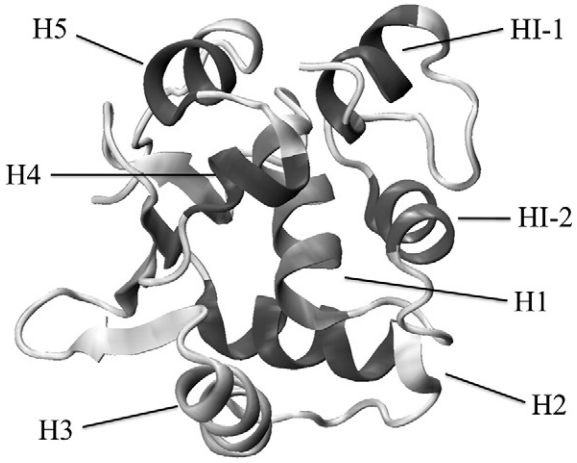

Fig. 1. Structure of apo Ets-1. Helices are shown in dark grey. The inhibitory module is formed by helices HI-1, HI-2, H4 and H5.

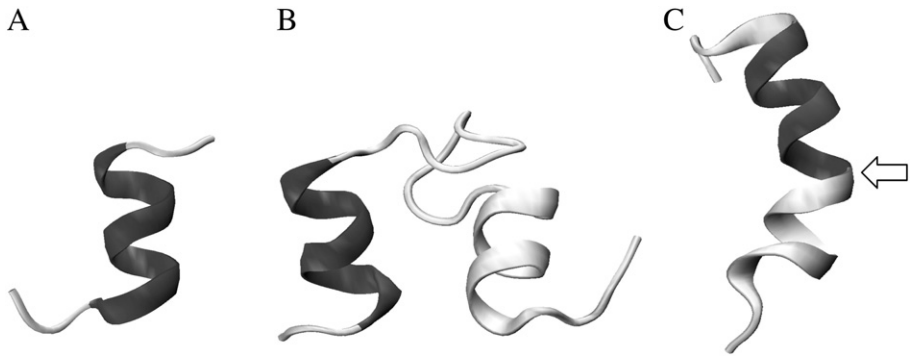

Fig. 2. Ets-1 constructs studied with REX. HI-1 is shown in dark grey. (a) HI-1. (b) HI-1 + HI-2. (c) HI-1 + H4. The arrow points to the GT linker that connects HI-1 and H4. This linker was used to mimic the arrangement of the helices in Δ301.

was mostly observed in structures with residues 306 to 310 in a helical conformation, but also in structures with a turn between residues 304 to 307. In the folded state, F304 and R309 form contacts with V308 and K305, respectively, which stabilize the helix.

To investigate the importance of the F304–R309 contact in stabilizing the unfolded state, we decided to perform simulations of the F304V + R309L double mutant. This mutant was chosen in order to preserve the overall hydrophobicity of the residues, and to retain the overall helical propensity of the construct (the helical propensities of F and V are 0.54 and 0.61, respectively, while the helical propensity of R and L is 0.21 [47]); therefore, the mutation only introduced geometrical effects. The simulations showed that the unfolded state is indeed destabilized in the mutant. Contacts between residues 304 and 309 occurred less frequently in the unfolded state, and the free energy of the unfolded state in terms of the helical fraction was decreased by 4.4 kJ/mol, making the mutant folded state slightly more favorable than the unfolded state. The mutant unfolded state favored partial π-helical structures over sheet or loop structures. Contacts between residues 304 and 308 were diminished in the folded state of the mutant. In the folded state, F304V was more frequently observed to interact with R309L, stabilizing π-helical conformers.

The importance of the F304–R309 contact for the unfolded state, and our strategy to stabilize the folded state by destabilizing the unfolded state was verified in simulations of apo Ets-1 Δ301. In accordance with experiments, in the wild-type HI-1 was preferentially folded. The free energy of the partially unfolded state of the protein (with HI-1 unfolded) was 4.2 kJ/mol higher than that of the folded state, which is somewhat below the estimate based on experimental hydrogen exchange protection factors of ~6.7 kJ/mol [31]. In the F304V + R309L mutant, the free energy of the unfolded state was increased by 3.7 kJ/mol, and contacts between residues 304 and 309 were less frequently observed in the partially unfolded state.

The presence of HI-2 significantly increased the stability of the folded state of HI-1, with the folded state 3.8 kJ/mol more stable than the unfolded state. In the folded state, significant hydrophobic contacts are made between F304, Y307, and Y329 (Fig. 4), while in the unfolded state frequent contacts are observed between Y307 and K316, and F304 and K318. To test the importance of the F304/Y307/Y329 contacts for the folded state, simulations were performed on a F304A + Y307A mutant of the HI-1 + HI-2 construct, as well as a F304V + Y307V mutant. The latter mutant has similar helical propensities as the wild type (the helical propensities of F, Y, and V are 0.54, 0.53, and 0.61, respectively) and retains the hydrophobic character of the residues, so the mutation only introduced geometrical effects. Simulations of the mutant showed that the folded state was destabilized by 3.3 kJ/mol in the F304A + Y307A mutant, and by 2.2 kJ/mol in the F304V + Y307V mutant, although in both constructs the folded state remained the most favorable. Simulations of the apo Ets-1 Δ301 showed that the folded state became destabilized by 1.3 and 1.7 kJ/mol for F304A + Y307A and F304V + Y307V mutants respectively.

While both mutants destabilize the folded state, there are marked differences in the mechanism by which this destabilization is achieved. Consistent with the fact that alanine has the highest helix propensity of all amino acids, the F304A + Y307A mutant showed more helical structure than the F304V + Y307V mutant. However, due to the small size of Ala, the F304A + Y307A mutant had a diminished ability to interact with other side chains, leading to a decrease in 304/307/329 interactions and an overall destabilization of the F304A + Y307A mutant compared to the wild type. Valine on the other hand, has a larger hydrophobic side chain, and the F304V + Y307V mutant interacted with the other side chains much more frequently than F304A + Y307A. Due to the lack of aromatic side chains however, interactions between residues 304/307/329 were less frequently observed than in the wild type. Therefore, consistent with its lower helical propensity, the helical state of HI-1 was less populated than in the wild type. The destabilizing effect of both mutants was lower in Δ301 than in the HI-1 + HI-2 constructs. In Δ301 stabilizing interactions between HI-1 and H4 (see below) partly counteracted the mutations, leading to a weaker overall destabilization of the mutants in the protein.

Simulations of the HI-1 + H4 construct showed that H4 had a positive effect on the stability of the folded state of HI-1. The folded state

Table 1
Free energies of the HI-1 folded state relative to the unfolded state[a].

System	Wild-type	F304V + R309L	F304A + Y307A	F304V + Y307V
HI-1[b]	3.2 ± 0.3	−1.2 ± 0.3		
HI-1 + HI-2[b]	−3.8 ± 0.3		−0.5 ± 0.2	−1.6 ± 0.3
HI-1 + H4 (unrestr.)[b,c]	−0.6 ± 0.3			
HI-1 + H4 (restr.)[b,d]	−2.9 ± 0.2			
Δ301[e]	−4.2 ± 0.1	−7.9 ± 0.1	−2.9 ± 0.1	−2.5 ± 0.1

a. In kJ/mol. The free energies of all unfolded states are at 0.0 kJ/mol; free energies were calculated using the helical fraction as reaction coordinate.
b. Standard deviations calculated from WHAM [43].
c. Using no restraints on H4.
d. Using backbone restraints on H4 in order to keep it helical.
e. Standard deviations calculated from bootstrapping [49].

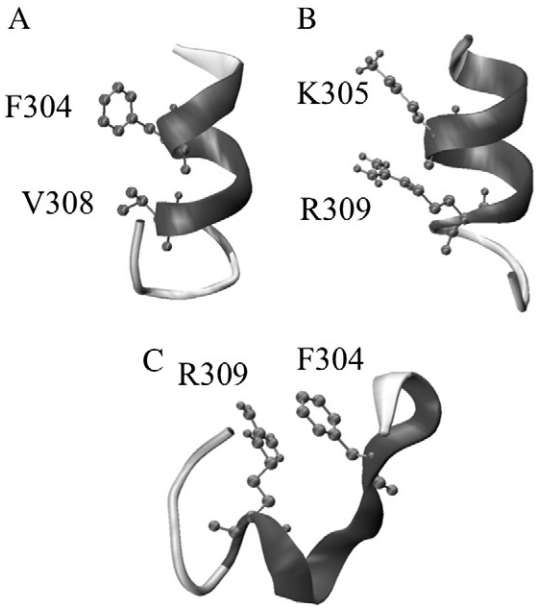

Fig. 3. Contacts observed in REX simulations of the constructs. (a) Folded state contact F304 + V308. (b) Folded state contact K305 + R309. (c) Unfolded state contact F304 + R309.

became slightly more stable than the unfolded state (by 0.6 kJ/mol). In the construct, the same F304–L421 and K305–L422 hydrogen bonds form as in apo Δ301. We observed that whenever these hydrogen bonds broke, the alignment between the H4 and HI-1 helices was disrupted, and HI-1 unfolded. The C terminus of HI-1 generally unfolded the fastest, while residues next to the linker remained helical through most of the simulations. From the simulations, we calculated that the likelihood of H4 and HI-1 folded at the same time is six times higher than the likelihood of HI-1 folded while H4 is unfolded. Our results indicate that the equilibrium is shifted towards structures with both helices HI-1 and H4 folded, and that the folded state of H4 stabilizes the folded state of HI-1.

To further verify the influence of H4 on the stability of HI-1 we performed simulations of the HI-1 + H4 construct in which the backbone of H4 was restrained to be helical. In these simulations the folded state was significantly more stable than the unfolded state, by 2.9 kJ/mol. The helix macrodipoles of HI-1 and H4 interacted favorably when both helices were folded, with an average interaction energy of −19.9 kJ/mol. Whenever the F304-L421 and K305–L422 hydrogen bonds between the helices broke, the alignment of helices was lost, leading to a loss of macrodipolar interaction (average of −4.6 kJ/mol), and the unfolding of HI-1. The magnitude of these interactions closely corresponded to those found in explicit water simulations of Δ301 [30]. These observations confirm the importance of macrodipolar and hydrogen bonding interactions between HI-1 and H4 for the stability of HI-1, and form additional evidence that disruptions of these interactions may lead to the unfolding of HI-1 in the protein [30].

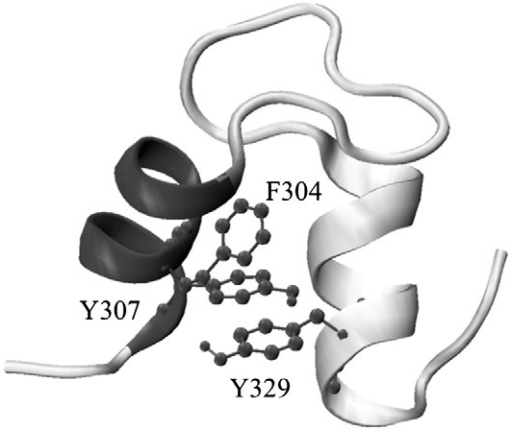

Fig. 4. Contacts between F304/Y307/Y329 in the folded state of the HI-1 + HI-2 construct as identified in REX simulations.

4. Discussion and Conclusion

Simulations of various Ets-1 HI-1 constructs showed the importance of local interactions for the stabilization of HI-1 in the apo state. The addition of HI-2 or H4 stabilized HI-1 by a similar amount of energy as observed in full-length Δ301. The stabilization by HI-2 results from specific hydrophobic contacts between F304, Y307 of HI-1, and Y329 of HI-2. The importance of these residues is in agreement with experimental mutation studies, that showed a large disruption in autoinhibition for F304A and Y307A mutations [31]. Stabilization of H4 is through macrodipolar and hydrogen bonding interactions with HI-1. Of particular interest is the F304V + R309L mutant, which stabilized the folded state of the protein. This stabilization is achieved through a destabilization of the unfolded state, and results from the removal of a favorable hydrophobic interaction between F304 and R309 in the unfolded state.

The simulation studies elucidated the factors that stabilize HI-1 in the apo state and help explain the loose packing of the helix in the protein. Our results suggest that the unfolding of Ets-1 upon DNA binding can be achieved by the removal of just a few local contacts, and does not require major rearrangements of the protein. Indeed, the backbone RMSD of Ets-1 residues 318–440 between the trimolecular Ets-1Δ280—Pax-5—DNA complex and apo Ets-1Δ300 was only 0.68 Å [31]; our data suggests that similar structural agreement will exist for the Ets-1Δ280—DNA complex not stabilized by Pax-5. The simulations provide further support for the central role of H4 for the autoinhibition/unfolding mechanism [23,29–31,48].

Acknowledgments

We thank Drs. Justin Spiriti, YingHua Chung, George Patargias and Hiqmet Kamberaj for discussions. Computer time was provided by the Teragrid and XSEDE, as well as USF Research Computing. This work was supported by NSF CAREER Award CHE-1007816.

References

[1] I.G. Maroulakou, D.B. Bowe, Expression and function of Ets transcription factors in mammalian development: a regulatory network, Oncogene 19 (2000) 6432–6442.
[2] K. Teruyama, M. Abe, T. Nakano, C. Iwasaka-Yagi, S. Takahashi, S. Yamada, Y. Sato, Role of transcription factor Ets-1 in the apoptosis of human vascular endothelial cells, Journal of Cellular Physiology 188 (2001) 243–252.
[3] E. Lelievre, F. Lionneton, F. Soncin, B. Vandenbunder, The Ets family contains transcriptional activators and repressors involved in angiogenesis, The International Journal of Biochemistry & Cell Biology 33 (2001) 391–407.
[4] P.N. Span, P. Manders, J.J. Heuvel, C.M.G. Thomas, R.R. Bosch, L.V. Beex, C.G.J. Sweep, Expression of the transcription factor Ets-1 is an independent prognostic marker for relapse-free survival in breast cancer, Oncogene 21 (2002) 8506–8509.
[5] D.W. Lincoln II, K. Bove, The transcription factor Ets-1 in breast cancer, Frontiers in Bioscience 10 (2005) 506–511.
[6] B. Davidson, R. Reich, I. Goldberg, W.H. Gotlieb, J. Kopolovic, A. Berner, G. Ben-Baruch, M. Bryne, J.M. Nestland, Ets-1 messenger RNA expression is a novel marker of poor survival in ovarian carcinoma, Clinical Cancer Research 7 (2001) 551–557.
[7] N. Takai, T. Miyazaki, M. Nishida, K. Nasu, I. Miyakawa, c-Ets1 is a promising marker in epithelial ovarian cancer, International Journal of Molecular Medicine 9 (2002) 287–292.
[8] J. Fujimoto, I. Aoki, H. Toyoki, S. Khatun, E. Sato, H. Sakaguchi, T. Tamaya, Clinical implications of expression of ETS-1 related to angiogenesis in metastatic lesions of ovarian cancer, Oncology 66 (2004) 420–428.
[9] J. Fujimoto, I. Aoki, H. Toyoki, S. Khatun, T. Tamaya, Clinical implications of expression of ETS-1 related to angiogenesis in uterine cervical cancers, Annals of Oncology 13 (2002) 1598–1604.
[10] H. Sasaki, H. Yukiue, S. Moiriyama, Y. Kobayashi, Y. Nakashima, M. Kaji, M. Kiriyama, I. Fukai, Y. Yamakawa, Y. Fujii, Clinical significance of matrix metalloproteinase-7 and Ets-1 gene expression in patients with lung cancer, Journal of Surgical Research 101 (2001) 242–247.

[11] K. Tokuhara, Y. Ogata, M. Nakagawa, K. Shirouzu, Ets-1 expression in vascular endothelial cells as an angiogenic and prognostic factor in colorectal carcinoma, International Surgery 88 (2003) 25–33.
[12] T. Ito, T. Nakayama, M. Ito, S. Naito, T. Kanematsu, I. Sekine, Expression of the ets-1 proto-oncogene in human pancreatic carcinoma, Modern Pathology 11 (1998) 209–215.
[13] T. Nakayama, M. Ito, A. Ohtsuru, S. Naito, M. Nakashima, I. Sekine, Expression of the ets-1 proto-oncogene in human thyroid tumor, Modern Pathology 12 (1999) 61–68.
[14] F. de Nigris, T. Mega, N. Berger, M.V. Barone, M. Santoro, G. Viglietto, P. Verde, A. Fusco, Induction of ETS-1 and ETS-2 transcription factors is required for thyroid cell transformation, Cancer Research 61 (2001) 2267–2275.
[15] S. Arora, J. Kaur, C. Sharma, M. Mathur, S. Bahadur, N.K. Shukla, S.V.S. Deo, R. Ralhan, Stromelysin 3, Ets-1, and vascular endothelial growth factor expression in oral precancerous and cancerous lesions: Correlation with microvessel density, progression, and prognosis, Clinical Cancer Research 11 (2005) 2272–2284.
[16] R.X. Leng, H.F. Pan, G.M. Chen, C.C. Feng, Y.G. Fan, D.Q. Ye, X.P. Li, The dual nature of Ets-1: Focus to the pathogenesis of systemic lupus erythematosus, Autoimmunity Reviews 10 (2011) 439–443.
[17] S.L. Meddle, P.M. Bull, G. Leng, J.A. Russell, M. Ludwig, Somatostatin Actions on Rat Supraoptic Nucleus Oxytocin and Vasopressin Neurones, Journal of Neuroendocrinology 22 (2010) 438–445.
[18] P.C. Hollenhorst, L.P. McIntosh, B.J. Graves, Genomic and Biochemical Insights into the Specificity of ETS Transcription Factors, Annual Review of Biochemistry vol 80 (80) (2011) 437–471.
[19] C. Wasylyk, A.P. Bradford, A. GutierrezHartmann, B. Wasylyk, Conserved mechanisms of Ras regulation of evolutionary related transcription factors, Ets1 and Pointed P2, Oncogene 14 (1997) 899–913.
[20] B.S. Yang, C.A. Hauser, G. Henkel, M.S. Colman, C. VanBeveren, K.J. Stacey, D.A. Hume, R.A. Maki, M.C. Ostrowski, Ras-mediated phosphorylation of a conserved threonine residue enhances the transactivation activities of c-Ets1 and c-Ets2, Molecular and Cellular Biology 16 (1996) 538–547.
[21] C.M. Slupsky, L.N. Gentile, L.W. Donaldson, C.D. Mackereth, J.J. Seidel, B.J. Graves, L.P. McIntosh, Structure of the Ets-1 pointed domain and mitogen-activated protein kinase phosphorylation site, Proceedings of the National Academy of Sciences of the United States of America 95 (1998) 12129–12134.
[22] A. Gegonne, B. Punyammalee, B. Rabault, R. Bosselut, S. Seneca, M. Crabeel, J. Ghysdael, Analysis of the DNA-Binding and Transcriptional Activation Properties of the Ets1 Oncoprotein, The New Biologist 4 (1992) 512–519.
[23] M.A. Pufall, B.J. Graves, Autoinhibitory domains: Modular effectors of cellular regulation, Annual Review of Cell and Developmental Biology 18 (2002) 421–462.
[24] G.M. Lee, M.A. Pufall, C.A. Meeker, H.S. Kang, B.J. Graves, L.P. McIntosh, The affinity of Ets-1 for DNA is modulated by phosphorylation through transient interactions of an unstructured region, Journal of Molecular Biology 382 (2008) 1014–1030.
[25] J. Hagman, R. Grosschedl, An Inhibitory Carboxyl-Terminal Domain in Ets-1 and Ets-2 Mediates Differential Binding of Ets Family Factors to Promoter Sequences of the Mb-1 Gene, Proceedings of the National Academy of Sciences of the United States of America 89 (1992) 8889–8893.
[26] C. Wasylyk, J.P. Kerckaert, B. Wasylyk, A Novel Modulator Domain of Ets Transcription Factors, Genes & Development 6 (1992) 965–974.
[27] M.D. Jonsen, J.M. Petersen, Q.P. Xu, B.J. Graves, Characterization of the cooperative function of inhibitory sequences in Ets-1, Molecular and Cellular Biology 16 (1996) 2065–2073.
[28] B. Rabault, J. Ghysdael, Calcium-Induced Phosphorylation of Ets1 Inhibits Its Specific DNA-Binding Activity, Journal of Biological Chemistry 269 (1994) 28143–28151.
[29] C.W. Garvie, M.A. Pufall, B.J. Graves, C. Wolberger, Structural analysis of the autoinhibition of Ets-1 and its role in protein partnerships, Journal of Biological Chemistry 277 (2002) 45529–45536.
[30] H. Kamberaj, A. van der Vaart, Correlated motions and interactions at the onset of the DNA-induced partial unfolding of Ets-1, Biophysical Journal 96 (2009) 1307–1317.
[31] G.M. Lee, L.W. Donaldson, M.A. Pufall, H.S. Kang, I. Pot, B.J. Graves, L.P. McIntosh, The structural and dynamic basis of Ets-1 DNA binding autoinhibition, Journal of Biological Chemistry 280 (2005) 7088–7099.
[32] H. Wang, L.P. McIntosh, B.J. Graves, Inhibitory module of Ets-1 allosterically regulates DNA binding through a dipole-facilitated phosphate contact, Journal of Biological Chemistry 277 (2002) 2225–2233.
[33] H. Kamberaj, A. van der Vaart, Extracting the causality of correlated motions from molecular dynamics simulations, Biophysical Journal 97 (2009) 1747–1755.
[34] J.M. Petersen, J.J. Skalicky, L.W. Donaldson, L.P. McIntosh, T. Alber, B.J. Graves, Modulation of transcription factor Ets-1 DNA binding: DNA-induced unfolding of an α helix, Science 269 (1995) 1866–1869.
[35] E. Neria, S. Fischer, M. Karplus, Simulation of activation free energies in molecular systems, Journal of Chemical Physics 105 (1996) 1902–1921.
[36] U. Haberthur, A. Caflisch, FACTS: Fast analytical continuum treatment of solvation, Journal of Computational Chemistry 29 (2008) 701–715.
[37] B.R. Brooks, C.L. Brooks III, A.D. MacKerell Jr., L. Nilsson, R.J. Petrella, B. Roux, Y. Won, G. Archontis, C. Bartels, S. Boresch, A. Caflisch, L. Caves, Q. Cui, A.R. Dinner, M. Feig, S. Fischer, J. Gao, M. Hodoscek, W. Im, K. Kuczera, T. Lazaridis, J. Ma, V. Ovchinnikov, E. Paci, R.W. Pastor, C.B. Post, J.Z. Pu, M. Schaefer, B. Tidor, R.M. Venable, H.L. Woodcock, X. Wu, W. Yang, D.M. York, M. Karplus, CHARMM: The biomolecular simulation program, Journal of Computational Chemistry 30 (2009) 1545–1614.
[38] J.P. Ryckaert, G. Ciccotti, H.J.C. Berendsen, Numerical integration of the Cartesian equations of motion of a system with constraints: Molecular dynamics of n-alkanes, Journal of Computational Physics 23 (1977) 327–341.
[39] Y. Sugita, Y. Okamoto, Replica-exchange molecular dynamics method for protein folding, Chemical Physics Letters 314 (1999) 141–151.
[40] D.J. Sindhikara, D.J. Emerson, A.E. Roitberg, Exchange Often and Properly in Replica Exchange Molecular Dynamics, Journal of Chemical Theory and Computation 6 (2010) 2804–2808.
[41] D. Frishman, P. Argos, Knowledge-based protein secondary structure assignment, Proteins: Structure, Function, and Genetics 23 (1995) 566–579.
[42] A.M. Ferrenberg, R.H. Swendsen, Optimized Monte-Carlo Data-Analysis, Physical Review Letters 63 (1989) 1195–1198.
[43] J.D. Chodera, W.C. Swope, J.W. Pitera, C. Seok, K.A. Dill, Use of the weighted histogram analysis method for the analysis of simulated and parallel tempering simulations, Journal of Chemical Theory and Computation 3 (2007) 26–41.
[44] M. Seeber, A. Felline, F. Raimondi, S. Muff, R. Friedman, F. Rao, A. Caflisch, F. Fanelli, Wordom: A User-Friendly Program for the Analysis of Molecular Structures, Trajectories, and Free Energy Surfaces, Journal of Computational Chemistry 32 (2011) 1183–1194.
[45] W. Humphrey, A. Dalke, K. Schulten, VMD: Visual molecular dynamics, Journal of Molecular Graphics 14 (1996) 33.
[46] J.M. Scholtz, R.L. Baldwin, The Mechanism of Alpha-Helix Formation by Peptides, Annual Review of Biophysics and Biomolecular Structure 21 (1992) 95–118.
[47] C.N. Pace, J.M. Scholtz, A helix propensity scale based on experimental studies of peptides and proteins, Biophysical Journal 75 (1998) 422–427.
[48] P.C. Hollenhorst, M.W. Ferris, M.A. Hull, H. Chae, S. Kim, B.J. Graves, Oncogenic ETS proteins mimic activated RAS/MAPK signaling in prostate cells, Genes & Development 25 (2011) 2147–2157.
[49] B. Efron, Jackknife, Bootstrap and Other Resampling Methods in Regression-Analysis - Discussion, The Annals of Statistics 14 (1986) 1301–1304.